

# 5kW Hall Thruster Coupling Test: High-Power Operation and Performance Optimization

IEPC-2025-482

*Presented at the 39th International Electric Propulsion Conference  
Imperial College London • London, United Kingdom  
14-19 September 2025*

Steven Ward<sup>1</sup>, Joseph Pawelski<sup>2</sup>, Jan Walter Schroeder<sup>3</sup>  
*CisLunar Industries, 815 14th St SW, D100, Loveland, CO 80537, USA*

Olivier Duchemin<sup>4</sup>  
*Safran Spacecraft Propulsion, 1 Av. Hubert Curien, 27200 Vernon, France*

Mitchell Walker<sup>5</sup>, Julian Lopez-Uricoechea<sup>6</sup>, Richeek Dutta<sup>7</sup>, Dan Lev<sup>8</sup>,  
*Georgia Institute of Technology, North Avenue NW, Atlanta, GA 30332, USA*

**Abstract:** This work details the successful integration and testing of the CisLunar Modular Power Processing Unit (Mod PPU-6000) with the Safran PPS®5000 Hall Effect Thruster at the Georgia Institute of Technology High Power Electric Propulsion Laboratory. The goal of the test campaign was to verify the compatibility and performance of the PPU and thruster across a range of operational modes, as well as to characterize thrust and specific impulse at various power levels, and to validate various startup sequences. The Mod PPU-6000 supplied up to 7 kW with a voltage range of 300-700V to the PPS®5000. 17 operating were performed in a vacuum chamber with a thrust stand, and a Faraday probe, and a Langmuir probe for diagnostics. Two gases, Xenon and Krypton were used. On Xenon, thrust ranged from 50 mN to 375 mN with Isp from 1248 s to 2472 s, while Krypton achieved up to 311 mN and Isp of 2522 s. Operation at 600 V demonstrated stable high-efficiency mode with low discharge oscillations. In a previously untested sustain mode the thruster was stable. The results showed that the combined system is very robust and versatile and suitable for future high-power, high-efficiency electric propulsion missions.

---

<sup>1</sup> Chief Engineer

<sup>2</sup> Chief Technology Officer

<sup>3</sup> Chief Product Officer, walter@cislunarindustries.com

<sup>4</sup> Chief Engineer, olivier.duchemin@safrangroup.com

<sup>5</sup> Professor, Aerospace Engineering, mitchell.walker@coe.gatech.edu

<sup>6</sup> Research assistant, jlopezur3@gatech.edu

<sup>7</sup> Research assistant, rdutta46@gatech.edu

<sup>8</sup> Research Engineer, High Power Electric Propulsion Lab, dan.lev@gatech.edu



## Nomenclature

<i>A</i>	= amplitude of oscillation
<i>ADC</i>	= Analog-to-Digital Converter
<i>CAN</i>	= Controller Area Network
<i>CFM</i>	= Cubic Feet per Minute (pump flow rate)
<i>DAC</i>	= Digital-to-Analog Converter
<i>f<sub>max</sub></i>	= frequency of dominant discharge current oscillation (FFT peak)
<i>GaN</i>	= Gallium Nitride
<i>HET</i>	= Hall Effect Thruster
<i>HPEPL</i>	= High-Power Electric Propulsion Laboratory (Georgia Tech)
<i>I<sub>b,co</sub></i>	= ion beam current (background pressure corrected)
<i>I<sub>b,un</sub></i>	= ion beam current (uncorrected for background pressure)
<i>I<sub>d</sub></i>	= discharge current
<i>I<sub>d,p2p</sub></i>	= peak-to-peak discharge current oscillation
<i>I<sub>d,rms</sub></i>	= RMS of discharge current fluctuations
<i>IM</i>	= magnet current
<i>I<sub>sp</sub></i>	= specific impulse
<i>LET</i>	= Linear Energy Transfer
<i>LN<sub>2</sub></i>	= Liquid Nitrogen
<i>MCU</i>	= Microcontroller Unit
<i>m</i>	= propellant mass flow rate
<i>PB</i>	= background chamber pressure
<i>PFCV</i>	= Propellant Flow Control Valve
<i>P<sub>d</sub></i>	= discharge power
<i>PMA</i>	= Propellant Management Assembly
<i>PPU</i>	= Power Processing Unit
<i>PWM</i>	= Pulse-Width Modulation
<i>PPS®5000</i>	= Safran 5 kW Hall Effect Thruster
<i>SEE</i>	= Single Event Effect
<i>Si</i>	= Silicon (semiconductor rectifier)
<i>T</i>	= thrust
<i>θ<sub>b,co</sub></i>	= ion beam divergence half-angle (background pressure corrected)
<i>θ<sub>b,un</sub></i>	= ion beam divergence half-angle (uncorrected)
<i>TID</i>	= Total Ionizing Dose
<i>UART</i>	= Universal Asynchronous Receiver/Transmitter
<i>VCO</i>	= Voltage-Controlled Oscillator
<i>V<sub>d</sub></i>	= discharge voltage
<i>VTF-2</i>	= Vacuum Test Facility 2 (Georgia Tech)
<i>ZVS</i>	= Zero-Voltage Switching

## I. Introduction

### A. Background

The PPS®5000 is a 5-kW-class Hall Effect thruster (HET) designed by Safran, which first flew on a mission in 2021. It has since been flown and produced in increasing numbers confirming an increasing demand of the 5-kW-class HET.

This report documents the results of the integration and testing of the CisLunar Modular Power Processing Unit (Mod PPU-6000) with the Safran PPS®5000 Hall Effect Thruster at the Georgia Institute of Technology High Power Electric Propulsion Laboratory. The goal of the test campaign was to verify the compatibility and performance of the PPU and thruster across a range of operational modes. The primary objectives were to:

1. Verify the interaction between the CisLunar Mod PPU-6000 and the Safran PPS®5000 thruster.



2. Validate the PPU's performance across operational modes.
3. Characterize thrust and specific impulse at various power levels.
4. Validate various startup sequences for the integrated system.

## B. Previous work

The PPU6000 is built on a modular gallium nitride (GaN) resonant converter topology that enables discharge power supply up to 7 kW with high efficiency exceeding 97% across a broad range of input and output voltages. This architecture offers notable improvements in size and weight compared to older converter designs and supports configurable operation modes for either high current (300 V) or high voltage (600 V) applications.

Modular design in power processing units (PPUs) typically involves dividing the main discharge DC-DC converter into multiple identical modules, each capable of handling a fixed maximum current. These modules are replicated as needed to meet the total discharge current requirement. While this approach may slightly increase the overall volume of the PPU, it offers several advantages over conventional single-module designs. One key benefit is scalability: propulsion systems can be adapted to different thruster power levels simply by adding or removing modules, eliminating the need for custom PPU designs and reducing the associated design, manufacturing, and qualification efforts. Once a module is qualified, it can be reused across multiple systems, streamlining the development process.

Reliability is also enhanced in modular systems. Traditional PPUs often require full duplication of the discharge module to ensure redundancy, which nearly doubles the system mass. In contrast, modular designs can achieve similar or better reliability by adding only one or two backup modules. Although the reliability of a system with  $N$  modules, each with reliability  $P$ , is approximately  $N \times P$ , the inclusion of spare modules significantly improves overall reliability with minimal mass penalty.

Several PPUs have successfully implemented modular architectures. NASA developed a system based on 500 W converter modules operating at 50 kHz and capable of up to 400 VDC, supporting various thruster startup modes<sup>1</sup>. Thales Alenia Space Belgium designed the Mk3 PPU using two 2.5 kW modules in parallel to deliver up to 4.74 kW, with the power limit imposed to manage inrush current during ignition<sup>2</sup>. Rafael adopted a modular approach for the electric propulsion system of the Vents satellite, using four active modules to deliver 600 W of discharge power and four additional backup modules to ensure high mission reliability<sup>3</sup>.

The Cislunar PPU is among the few modular systems exceeding 5 kW. Thales Alenia Space Belgium qualified a 5 kW modular PPU that was tested with the SPT-140D Hall thruster at voltages up to 400 V and power levels up to 4.7 kW<sup>4</sup>. This system is now flight-proven. Maxar's 6 kW PPU supports both the BHT-6000 and the 12 kW AEPS Hall thrusters. For AEPS, two PPUs are connected in parallel to meet the required discharge current<sup>5</sup>. Maxar also developed an extended-range version of the same PPU to power the SPT-140 Hall thruster on the Psyche mission, accommodating the wide power range of the thruster as available solar power diminishes with increasing distance from the Sun, down to approximately 1 kW<sup>6</sup>.

Compared to most of the previously discussed examples, the Cislunar PPU6000 offers a notably wide operational range. It is capable of reaching output voltages up to 600 V, addressing the growing demand for Hall thrusters to achieve specific impulse values exceeding 2,000 seconds. At the same time, the PPU maintains high conversion efficiency even when operating at lower power levels, down to 1 kW, making it suitable for a broad spectrum of thruster configurations without compromising performance.



## II. Materials and Methods

### A. Power Processing Unit and Thruster

#### 1. *CisLunar Mod PPU-6000*

The CisLunar Mod PPU-6000 (Fig. 1) was used in this experiment. It is a 6kW power supply to support the operating range of the BHT-6000 and PPS5000 Hall Thrusters at 300V - 600V with an unregulated bus voltage of 96-128VDC with output power up to 7kW. The PPU design is built upon the CisLunar Industries patented modular configurable electric power conversion technology which features a plurality of anode and auxiliary supplies. The power modules utilize resonate circuit topologies and Zero-Voltage Switching (ZVS) with GaN high electron mobility transistors for 97% conversion efficiencies and severe radiation tolerance.

The auxiliary PPU supplies support operation of the Propellant Feed Control Valve (PFCV) and Xenon Flow Control (XFC) for both proportional valve and thermal throttle designs.

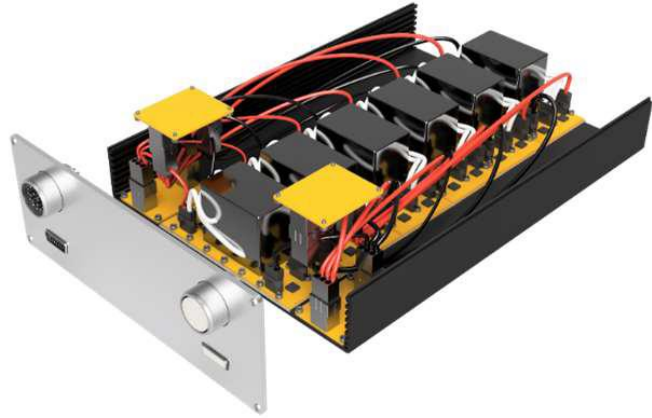


**Figure 1. Flight CisLunar Mod PPU-6000**  
(Render based on tested brass-board design)

**Table 1. Configurations of the CisLunar Mod PPU-6000**

Configuration	Vout (min, V)	Vout (max, V)	Iout (@Vmin, A)	Iout (@Vmax, A)	Pout (max, W @>117VDC in)
Series	300	600	15	11.33	6800
Parallel	150	300	30	22.67	6800

#### 2. *PPU Description and Background*

The CisLunar PPU6000 was designed to meet a 18mo development timeline for a commercial Orbital Transfer Vehicle. Most of the components are “flight-like”, being either supplied as radiation hardened, or are equivalent to components that have been tested for Single Event Effects (SEE) and shown to be robust. This PPU is a development model, constructed with custom brass-board power modules controlled from a Microchip development board. Individual anode supply modules were tested in a thermal vacuum chamber at 133% operating voltage from -50C to 110C and measured a +9C max delta on the transformer. Development PPU mass is 10.4kg with overall dimensions of 415mm x 450mm x 100mm.





**Figure 2. PPU Development Unit** – Top section shows 6 Anode Converters. Lower left section shows Keeper, Magnet and Heater supplies, with Ignitor and Throttle drivers as proto-board type build. Lower right is the Microchip RH707 EVK and a USB to serial converter for communication with a laptop (not shown). Figure is partially blurred due to export restrictions.

### 3. Power Bus Requirements

The PPU is designed to take 2 power inputs, a primary power supply of 96-128VDC (full 6kW performance at >110VDC and 7kW capable with >118VDC) and a secondary supply of 28V, <4A. The controls are supplied from 28V, so the PPU will not communicate to the satellite without this power present.

For ground testing, a bank of 3x Meanwell CSP-300-120 (120V, 3kW output) power converters serve for the primary bus, and were set to 117VDC during the test. 28VDC was supplied from a TDK AC/DC type power supply.

### 4. Digital Controller

The PPU is controlled by a Microchip SAMRH707 Micro Controller Unit (MCU). The device has many options for communications, including SpaceWire, 1553, but currently we use either UART or CAN.

The MCU has Analog to Digital (ADC) and Digital to Analog (DAC) peripherals that are used for feedback control of the power converters. There are many PWM and Timer Counter modules that are used as well for direct control of the power conversion hardware. The anode converter uses a separate Voltage Controlled Oscillator (VCO) circuit which is controlled via DAC outputs, to achieve finer frequency resolution. There is some other digital logic associated with creating the interleaved switching commands for the anode converter groups (this PPU uses 3 phases of anode converters interleaved by 120 degrees).

The MCU controls all the power converters within the PPU: anode, magnet, heater, ignitor, keeper, thermothrottle, and valves.

During the coupling test, a laptop is used for command and telemetry. The controller can work in an automatic mode, or a fully manual mode. Manual mode was used for this testing to provide maximum control and flexibility of operation.





### 5. Anode Converter Modules

The variable 96-128V bus is converted to a variable DC output ranging from 150-300VDC via the anode modules. The anode supply is voltage controlled with fast and programmable current limiting. The 6kW PPU contains 6 modules grouped as 2 sets of 3-phase interleaved converters. The outputs of the 2 groups can be connected in series or parallel allowing 6kW operation at 600V or 300V (see Tab.2). Performance is reduced at 96V-112V input. The following table shows the Anode converter capabilities with >117V input. Max power is reduced to 5kW at 96V.

The converter uses variable switching frequency as control from the MCU, which provides the necessary gain scheduling.

An engineering model anode converter module has been previously tested in vacuum at 350V and 1.4kW to look at thermal performance at high power and high baseplate temperature of 100 degrees Celsius. The highest temperature delta was recorded at 9 degrees above baseplate temperature on the transformer.

The power diodes are surface mount devices, and their heat is conducted through the PCB, and TIM to reach the baseplate, yet their temperature delta is not excessive. The anode converter peak efficiency is 97.5% and maintains >95% efficiency over the full operating range.

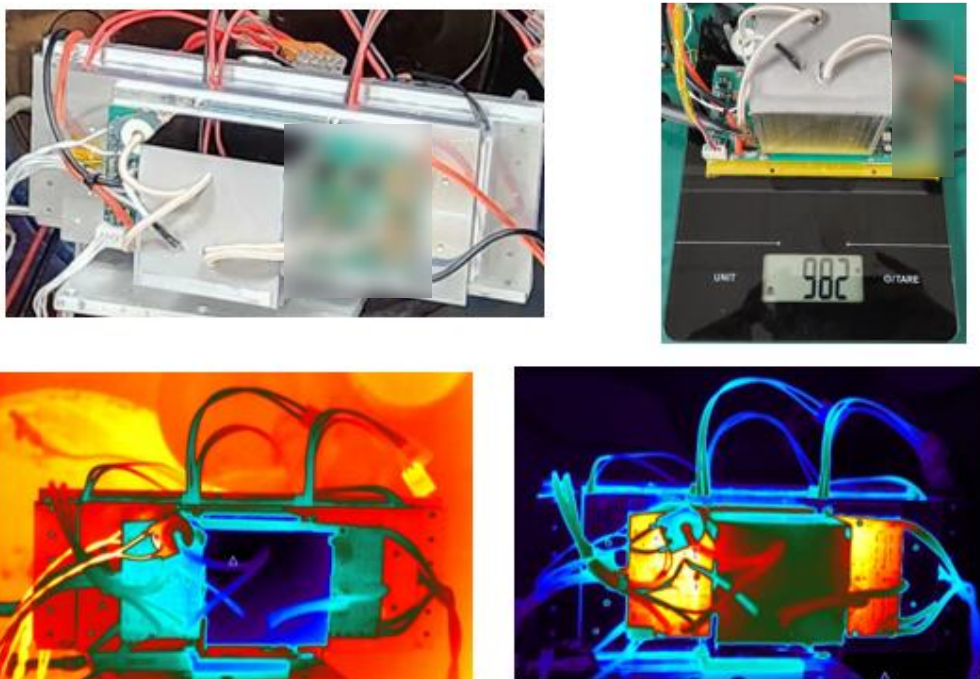


**Figure 3. TVAC testing of anode supply module**

### 6. Magnet Supply

There is a single, isolated, magnet power supply which is fed from the high voltage (96-128V) bus. A resonant converter is used with variable switching frequency, controlled directly from the MCU. The magnet supply has voltage feedback to the MCU.

### 7. Heater Supply

The heater supply is nearly identical to the magnet supply, providing isolated conversion from the high voltage bus. The heater supply is current controlled and has a programmable rate of current rise as well as voltage feedback.



#### 8. Keeper / Ignitor

There are 2 power converters used for the different operating modes of the keeper. A pulse-capable ignitor module provides up to 550V at whatever pulse rate and duration desired. There is only voltage feedback for the ignitor, no current measurement.

The keeper supply is current controlled and also has programmable power limit and can supply up to 40VDC. This converter is similar to the magnet and heater supplies, being resonant with variable frequency control directly from the MCU. The keeper supply has voltage feedback.

#### 9. Thermostrottle and Valve Drivers

The PPS5000 uses a thermostrottle Xenon Flow Control (XFC). This supply is a flyback converter using the auxiliary 28V bus. This converter has no voltage feedback, only current (voltage estimate is available).

The gas flow controller usually has at least 2 control valves that open the flow to the cathode and anode. These valves are opened by applying 28V to the solenoid coil.

#### 10. PPS@5000

The PPS@5000, produced by Safran Spacecraft Propulsion, is a 5kW rated Hall Effect Thruster purposely designed for “all-electric” satellites. It can operate in high-thrust or high specific impulse mode, and offers an operating lifespan of about 20,000 hours. The thruster is used for orbital positioning and station-keeping duties for a wide range of telecom and navigation satellites, as well as exploration spacecraft. For reliable gas control the PPS@5000 XFC features a thermostrottle design. The PPS@5000 was fully qualified in 2021 and has significant flight heritage.

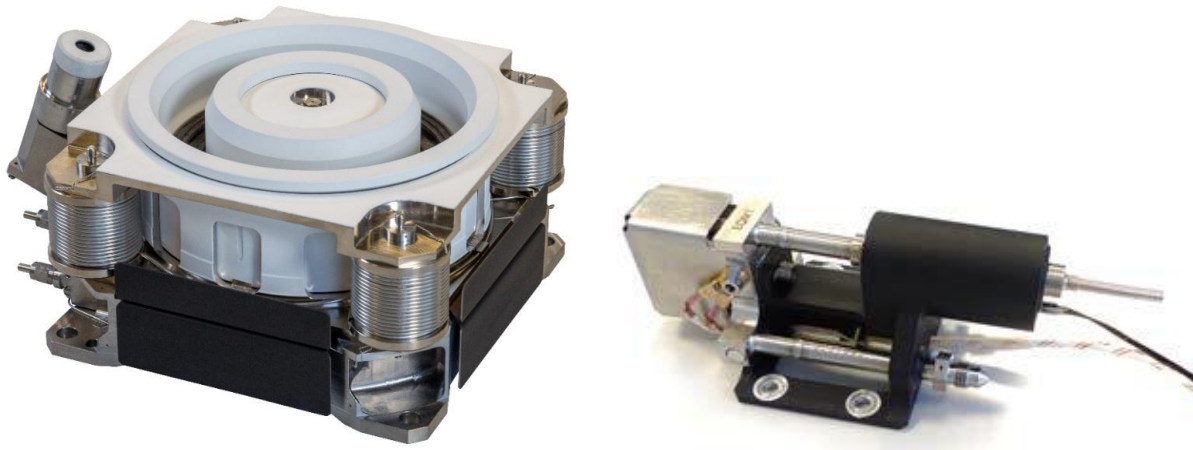


**Figure 4. PPS@5000 and Gas Flow Controller**

#### B. Test Facilities

The tests were conducted in Vacuum Test Facility 2 (VTF-2) at the Georgia Tech High-Power Electric Propulsion Laboratory. VTF-2 is 9.2 m long and 4.9 in diameter. A 495 CFM rotary-vane pump is used to reach 5 Torr, and a 3800 CFM blower is then used to reach rough vacuum of around 10 mTorr. Ten LN<sub>2</sub>-cooled CVI TMI reentrant cryopumps are used to reach high vacuum. At high vacuum, the chamber pressure was monitored with an Agilent Bayard-Alpert 571 hot-filament ion gauge on the side chamber. The Safran PPS@5000 was installed on the thruster stand inside the vacuum chamber along with the Safran Xenon Flow Controller (XFC). To ensure sufficient thermal management of the XFC it was installed on an aluminum plate of with a surface area  $\sim 100\text{cm}^2$ .



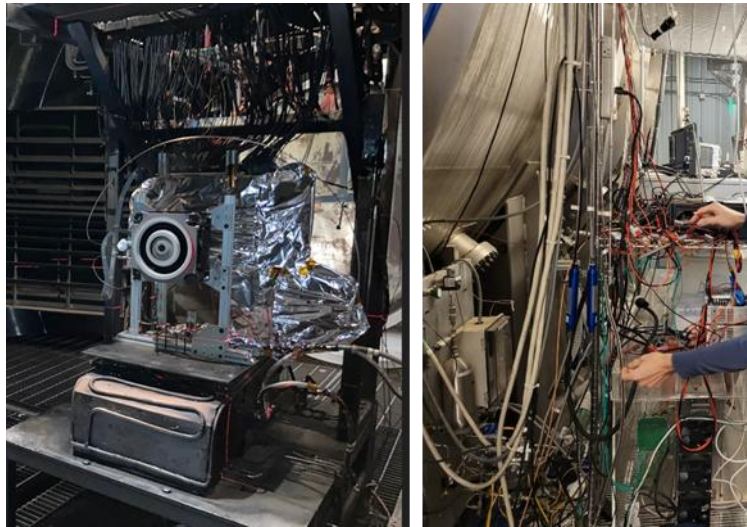


**Figure 5. Test stand**

The CisLunar Industries Mod PPU-6000 was installed outside the vacuum chamber. Existing wiring and waterfalls to the thrust stand were reused to connect the thruster and XFC to the PPU. Propulsion grade Xe and Kr were supplied from regulated bottles exterior of the chamber.

### **C. Test plan**

#### *1. Set points*

A total of 17 PPS@5000 setpoints were tested in Vacuum Test Facility 2 (VTF-2), with 14 of those being operated entirely on the PPU. Complete thruster operation on the PPU included controlling the thermal throttle on Safran's xenon flow controller (XFC). At each setpoint, we made thrust measurements, plume measurements, and discharge current oscillation measurements. VTF-2 achieved a base pressure of  $6.8 \times 10^{-9}$  Torr- $N_2$ , a minimum operating pressure of  $1.6 \times 10^{-6}$  Torr-Kr, and a maximum operating pressure of  $1.4 \times 10^{-5}$  Torr-Xe.

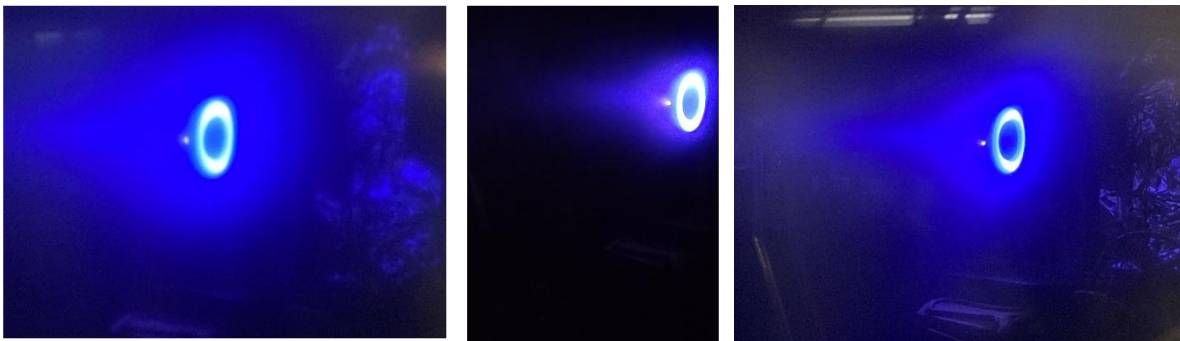


**Figure 6. System-level tests at various operational points.**

With the PPU, the PPS@5000 was operated on xenon and krypton at up to 7 kW and as low as 1 kW, covering high-thrust throttle points and high- $I_{sp}$  throttle points. The discharge voltage and discharge current supplied by the PPU ranged from 300 V to 600 V and from 3.33 A to 23.33 A, respectively.





## 2. Keeper “Sustain” Mode

A previously un-tested mode of operation for the PPS@5000 was tested near the end of the campaign. The thruster is put into a semi-idle “sustain” mode by engaging the keeper power supply while the anode discharge is active. Once the keeper discharge is detected, the anode supply is shut down, putting the thruster into sustain mode until ready to resume normal operation.

### D. Test matrix and global measurements

This section presents the operating setpoints and the corresponding global measurements, providing the baseline conditions for the subsequent performance analysis:

$P_d$  – discharge power  
 $V_d$  – discharge voltage  
 $I_d$  – DC discharge current  
 $I_M$  – magnet current  
 $P_B$  – background chamber pressure

The cathode flow fraction was a constant determined by the XFC.

To begin the test campaign, different elements of the thruster were powered with the lab supplies at HPEPL, then transitioned to full operation with the PPU. The column “Lab Supplies” in the table below refers to the thruster elements that were operated with the lab supplies.

The “Time of setpoint” column corresponds to the time of day at which the thruster achieved the corresponding setpoint (either from direct ignition or after ignition).

### E. Test matrix

The following test matrix lists the operating parameters investigated during the campaign.

$T$  – thrust  
 $I_{sp}$  – specific impulse  
 $f_{max}$  – frequency of dominant peak in discharge current FFT  
 $I_{d,rms}$  – AC rms of discharge current fluctuations  
 $I_{d,p2p}$  – peak-to-peak of discharge current  
 $I_{b,un}$  – Ion beam current calculated without background pressure correction  
 $I_{b,co}$  – Ion beam current calculated with background pressure correction  
 $\theta_{b,un}$  – Ion beam divergence half-angle calculated without background pressure correction  
 $\theta_{b,co}$  – Ion beam divergence half-angle calculated with background pressure correction  
 $\eta_T$  – Total thruster efficiency

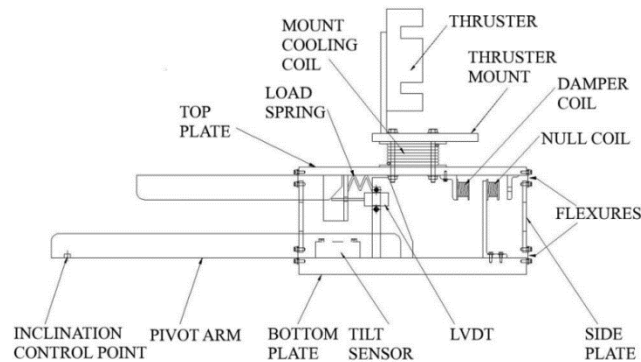


**Table 2. Test matrix**

Set-point	$\dot{m}$ (sccm)	$\dot{m}$ (mg/s)	Prop	$P_d$ (kW)	$V_d$ (V)	$I_d$ (A)	$I_M$ (A)	$P_B$ ( $\mu$ Torr)	Lab Supplies	Date	Time
1	140	8.7	Kr	3	300	10.00	5.5	4	All	11/19	14:33
2	140.5	8.7	Kr	3	300	10.00	5.5	3.9	-	11/19	16:54
3	218.3	13.5	Kr	5	300	16.67	6.5	6.3	All	11/19	17:06
4	170	10.6	Kr	5	400	12.50	6	4.5	Keeper, heater	11/20	11:18
5	142	8.8	Kr	6	600	10.00	6.5	3.8	-	11/20	13:22
6	58	3.6	Kr	1	300	3.33	3.5	1.6	-	11/20	14:45
7	163	10.1	Kr	7	600	11.67	6.5	4.3	-	11/20	13:45
8	249	15.5	Kr	6	300	20.00	6.5	7.5	-	11/20	17:48
9	284	17.6	Kr	7	300	23.33	6.5	8.8	-	11/20	18:30
10	42	4.1	Xe	1	300	3.33	3.6	2.2	-	11/21	11:49
11	177	17.3	Xe	5	300	16.67	7	8.3	-	11/21	13:03
12	203	19.8	Xe	6	300	20.00	7.4	13	-	11/21	13:55
13	228	22.2	Xe	7	300	23.33	7.8	14	-	11/21	14:44
14	141	13.8	Xe	5	400	12.50	6	8.2	-	11/21	15:39
15	111	10.8	Xe	6	600	10.00	7	6.9	-	11/21	16:29
16	120	11.7	Xe	7	600	11.67	7	7.3	-	11/21	17:20
17	71	6.9	Xe	2	300	6.67	4.6	4.1	-	11/21	18:19

**F. Test components****3. Thrust stand**

Each thrust measurement was calibrated by successively dropping three weights, weighing 10.8 g, 11.1 g, and 10.8 g. In the voltage traces of raw thrust data, initial voltage drop corresponds to thrust from turning the thruster off. We subsequently drop the weights and raise them back up to get a conversion of voltage to thrust. View raw thrust data for setpoint 2 as an example. A diagram of the null-type inverted pendulum thrust stand is shown below<sup>7</sup>.

**Figure 7. Thrust stand<sup>8</sup>****4. Faraday probe**

Calculations of beam current and divergence were done using methodology from Brown et al.<sup>8</sup> This method does not require prescribing a cutoff of 90% or 95% of the beam current to calculate the beam divergence and instead directly integrates the ion beam current and the axial ion beam current.

Background pressure correction was done by subtracting current at  $\pm 90^\circ$  from the entire sweep. The Faraday probe was swept in an  $180^\circ$  arc 1 m away from the thruster exit plane.



#### 5. *Langmuir probe*

Calculations of electron density and electron temperature were with the EEDF methodology from Lobbia and Beal<sup>9</sup>. We were not able to extract results from the Langmuir probe data with the thruster operating on krypton. When operating on xenon, we obtained Langmuir probe data in an 90° arc 1 m away from the thruster exit plane.

#### 6. *Time-lag phase portrait*

Time-lag phase portraits were constructed for the discharge current. The time lag was chosen as the smallest time lag that was a local minimum of the mutual information metric, as defined by Martin et al.<sup>10</sup>.

### **III. Results**

The integration and test campaign of the CisLunar Power Processing Unit (PPU) with the Safran PPS®5000 Hall Effect Thruster showed promising results summarized below. Detailed data, including thrust, specific impulse, and discharge characteristics, are presented below.



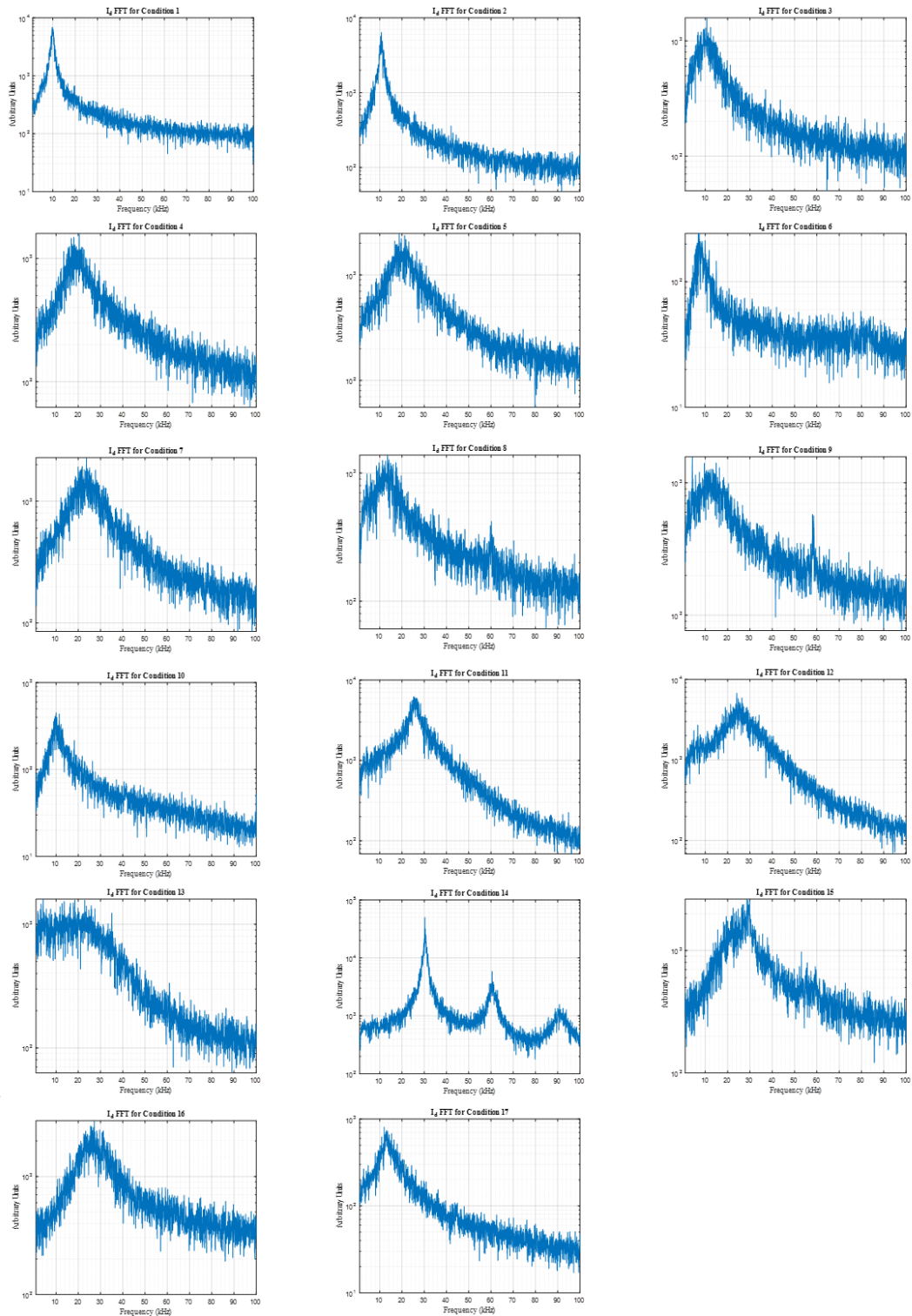


**Figure 8. Discharge current FFT spectrum for all test conditions.**





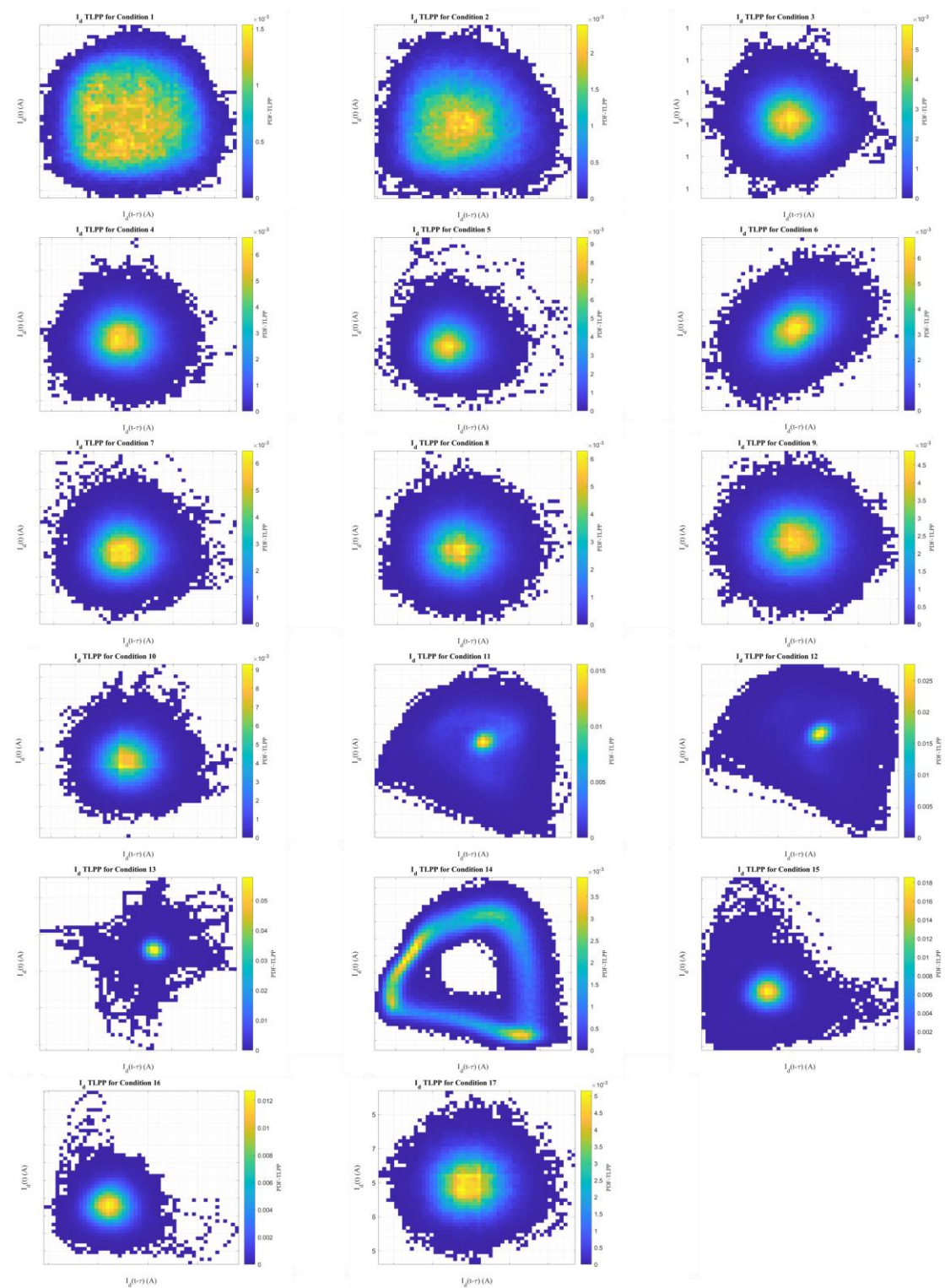


**Figure 9. Time-lag phase portraits (TLPP) of discharge current for all test conditions.**

### G. Impulse measurements

On xenon, thrust ranged from 50 mN to 375 mN, and the  $I_{sp}$  ranged from 1248 s to 2472 s. On krypton, thrust ranged from 39 mN to 311 mN, and the  $I_{sp}$  ranged from 1112 s to 2522 s. The thrust measurements throughout this report have an uncertainty of 3%.

### H. Key Highlights

Performance at extreme settings, including the 7 kW “turbo mode” and extended krypton tests, demonstrated the PPU's adaptability and robustness. The vacuum chamber achieved optimal operating pressures, ensuring test conditions were representative of actual mission environments.

### I. Global measurements

**Table 3. Global measurements**

Setpoint	$P_d$ (kW)	T (mN)	$I_{sp}$ (s)	$f_{max}$ (kHz)	$I_{d,rms}$ (A)	$I_{d,p2p}$ (A)	$\eta_T$ (%)
1	3	136	1598	9.8	1.2	6.6	36
2	3	134	1573	10.8	1.1	6.7	34
3	5	227	1713	10.7	0.6	4.5	38
4	5	207	1994	20.4	0.7	5.5	40
5	6	214	2478	18.8	1.0	8.6	43
6	1	39	1112	7.4	0.1	1.0	21
7	7	250	2522	23.7	1.0	8.5	44
8	6	270	1779	13.5	0.7	5.3	39
9	7	311	1801	11.6	0.7	5.6	39
10	1	50	1248	10	0.1	1.3	31
11	5	289	1704	25.2	2.3	17.5	48
12	6	338	1742	24.1	2.5	21.7	48
13	7	375	1723	22.6	0.9	17.8	45
14	5	258	1910	30.25	5.1	19.2	48
15	6	251	2369	28.7	1.3	13.5	49
16	7	284	2472	27.2	1.4	13.6	49
17	2	114	1693	13.1	0.3	2.2	47

Although beam current and divergence angle measurements were collected during the campaign, they are not included here, since the discussion focuses on thrust, specific impulse, efficiency, and discharge current oscillations as representative performance indicators.

### J. Keeper Sustain Mode

Telemetry data captured during the sustain mode shows the hand-off of cathode current from the anode to the keeper and then back to the anode (Fig 10)



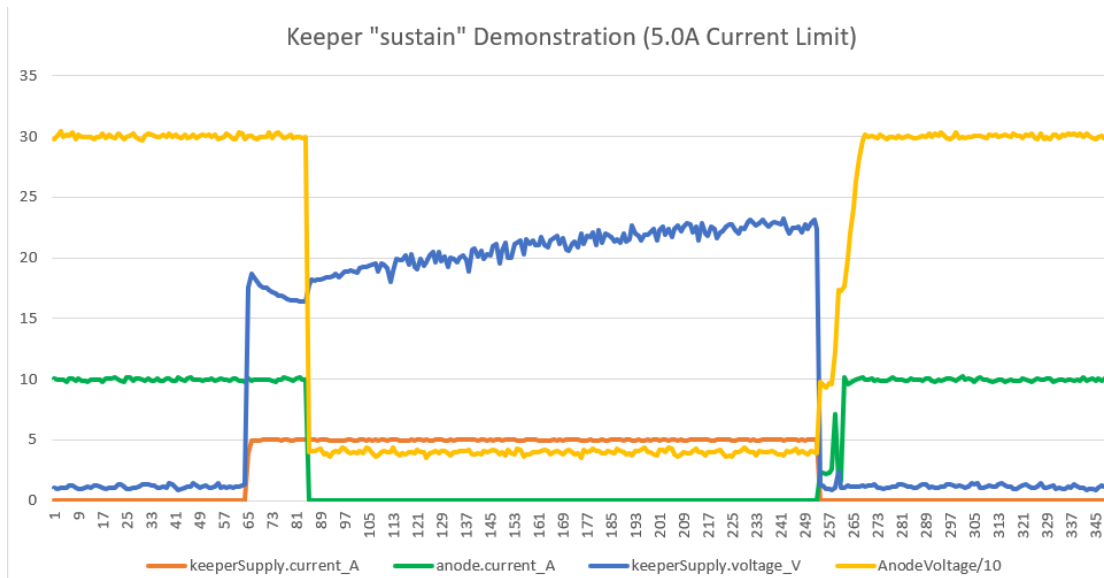


Figure 10. Telemetry data of Sustain Mode

## IV. Discussion

### A. Xenon Test Results

The thruster demonstrated stable and efficient performance across all tested power levels, ranging from 1 kW to 7 kW. Specific impulse (Isp) on xenon spanned from 1248 s at low-power settings to 2472 s at high-power settings, showcasing the system's versatility and adaptability.

Thrust levels reached up to 375 mN, with an uncertainty margin of  $\pm 3\%$ , confirming the accuracy of the setup.

### B. Krypton Test Results

Tests using krypton as a propellant revealed consistent operational trends, albeit with slightly reduced specific impulse compared to xenon. Isp ranged from 1112 s to 2522 s, reflecting the system's ability to handle alternative propellants efficiently. Thrust outputs were also robust, achieving up to 311 mN at high-power operating points.

### C. High Voltage Testing (600 V)

Preliminary high-voltage tests extended the operational envelope beyond the typical range, with promising results at 600 V discharge voltage. Stable discharge characteristics were observed, indicating the potential for higher-efficiency operations in future campaigns.

### D. Operational Stability

Across all power settings and propellants, the system maintained stability with low discharge current oscillations. The newly developed start-up sequence proved reliable, enabling smooth ignition and transitioning into steady-state operation.

### E. Keeper "Sustain" Mode

The keeper sustain mode was successfully tested. The idea was considered to speed up the rate at which we could take thrust data and resume operation. It also demonstrates a capability which may be useful for some missions if the anode gas supply could be turned off during the sustain period.



## V. Conclusion

In summary the coupling test between CisLunar Mod PPU-6000 and the Safran PPS®5000 Hall Effect Thruster demonstrated stable operation across a wide power range and with the two propellants, Xenon and Krypton operating from 1 kW to 7 kW, and at both 300 V and 600 V discharge voltages. The measured thrust ranged up to 375 mN on xenon (311 mN on krypton), with corresponding specific impulse values of 1248–2472 s (xenon) and 1112–2522 s (krypton). This validated the system’s performance. Multiple startup sequences and the newly tested “keeper sustain” mode, were successfully demonstrated. The results confirmed the compatibility of the two systems and validated key performance metrics. It also highlighted extended operational flexibility, supporting the readiness of this architecture for future high-efficiency electric propulsion missions.

## Acknowledgments

The authors would like to acknowledge the support of Georgia Tech personnel, as well as the contributions of CisLunar Industries and Safran personnel.

## References

- <sup>1</sup>National Aeronautics and Space Administration. *Power Processing Unit (PPU) for Small Spacecraft Electric Propulsion: Scalable PPU for Low-Power Hall Effect Thrusters*. NASA Glenn Research Center, LEW-TOPS-157, 2020.
- <sup>2</sup>Bourguignon, Eric, and Stéphane Fraselle. *Power Processing Unit Activities at Thales Alenia Space in Belgium*. Proceedings of the 36th International Electric Propulsion Conference, IEPC-2019-584, University of Vienna, Austria, 15–20 Sept. 2019.
- <sup>3</sup>Shoor, Boaz, et al. *The Rafael Power Processing Unit (PPU) for Electric Propulsion Systems*. Proceedings of the 36th International Electric Propulsion Conference, IEPC-2019-729, University of Vienna, Austria, 15–20 Sept. 2019.
- <sup>4</sup>Herman, Daniel A., et al. *Development and Qualification Status of the Electric Propulsion Systems for the NASA PPE Mission and Gateway Program*. Proceedings of the 37th International Electric Propulsion Conference, IEPC-2022-465, Boston, MA, United States, 19–23 June 2022.
- <sup>5</sup>Johnson, Ian, et al. *PPE Electric Propulsion Advancing to CDR: 12kW String*. Proceedings of the 37th International Electric Propulsion Conference, IEPC-2022-467, Massachusetts Institute of Technology, Cambridge, MA, United States, 19–23 June 2022.
- <sup>6</sup>Malone, Shane, et al. *Deep Space Power Processing Unit for the Psyche Mission*. Proceedings of the 36th International Electric Propulsion Conference, IEPC-2019-A280, University of Vienna, Austria, 15–20 Sept. 2019.
- <sup>7</sup>Xu, K. G., and Walker, M. L. R., “High-Power, Null-Type, Inverted Pendulum Thrust Stand,” *Review of Scientific Instruments* [online journal], Vol. 80, No. 5, Paper 055103, May 2009. URL: <https://doi.org/10.1063/1.3125626> [cited 4 September 2025].
- <sup>8</sup>Brown, D. L., Walker, M. L. R., Szabo, J., Huang, W., and Foster, J. E., “Recommended Practice for Use of Faraday Probes in Electric Propulsion Testing,” *Journal of Propulsion and Power* [online journal], Vol. 33, No. 3, May–June 2017, pp. 566–581. URL: [https://hpepl.ae.gatech.edu/sites/default/files/files/FaradayProbe\\_GuidelinesV33\\_No3\\_May\\_2017.pdf](https://hpepl.ae.gatech.edu/sites/default/files/files/FaradayProbe_GuidelinesV33_No3_May_2017.pdf) [cited 4 September 2025].
- <sup>9</sup>Lobbia, R. B., and Beal, B. E., “Recommended Practice for Use of Langmuir Probes in Electric Propulsion Testing,” *Journal of Propulsion and Power* [online journal], Vol. 33, No. 3, May–June 2017, pp. 566–581. DOI: 10.2514/1.B35531. URL: <https://doi.org/10.2514/1.B35531> [cited 4 September 2025].
- <sup>10</sup>Martin, R., Koo, J., and Eckhardt, D., “Impact of Embedding View on Cross Mapping Convergence,” *arXiv* [preprint], March 2019. DOI: 10.48550/arXiv.1903.03069. URL: <https://arxiv.org/pdf/1903.03069> [cited 4 September 2025].

